ARCHIVES OF CIVIL AND MECHANICAL ENGINEERING 18 (2018) 1547–1561

Available online at www.sciencedirect.com

ScienceDirect

journal homepage: http://www.elsevier.com/locate/acme

Original Research Article

Shear strength degradation of steel plate shear walls with optional located opening

Mohammad Jalilzadeh Afshari *, *Majid Gholhaki*

Faculty of Civil Engineering, Semnan University, Semnan, Iran

ARTICLE INFO

Article history:
Received 11 January 2018
Accepted 22 June 2018
Available online 29 July 2018

Keywords:
Steel plate shear wall
Shear strength
Finite element
Tension field
Opening

ABSTRACT

Regarding high ductility and potential of steel plate shear walls in energy absorption, they are required to be very thin in thickness especially in upper floors of the building in order to resist lateral loads and sometimes it will reach to a fraction of millimeter in calculations. Since preparation of such thin steel plates is not simply possible, a thicker plate with an opening can be used to reduce stiffness. On the other hand, the existence of opening is inevitable due to architectural considerations such as lighting. In the present paper, shear strength of steel plate shear wall with openings in different zones has been studied by finite element method. As a result, an empirical simple dimensionless equation has been presented to estimate accurately the amount of decrease of shear strength of the wall with an arbitrary opening position in any zone of the plate. To validate the accuracy of suggested relation, numerous finite element models have been simulated with different geometric properties such as shape, diameter, location of opening, thickness and span to height ratio of plate. Comparing results with that of suggested relation and corresponding values of theoretic relations shows the accuracy of the proposed relation for applying in a wide range of steel plate shear walls with different geometric specifications.

1. Introduction

In recent years, many experimental researches have been conducted on steel plate shear walls under monotonic and cyclic loads and results show high stiffness, sufficient strength, excellent ductility, high energy absorption and dissipation of this seismic resisting system. Concerning that steel plate shear walls (SPSWs)[1] are used in seismic rehabilitation of the structures in addition to newly constructed structures, researchers have been interested in analytical study of steel plate shear walls.

Sabouri Ghomi and Robertz studied experimentally the effect of opening on behavior of steel shear panels with embedment of circular openings in the center of the plate under cyclic loads [1]. To construct any panel, the steel plate was bolted to boundary members and horizontal and vertical boundary elements were bound via simple connections. Cyclic

* *Corresponding author at*: Unit 5, No. 6, 9th East Aseman Ave., Sadaat Abad, Tehran, Iran.
E-mail addresses: jalilzadeh.afshari@semnam.ac.ir, m_jalilzadeh.afshari@yahoo.com (M.J. Afshari), mgholhaki@semnan.ac.ir (M. Gholhaki).

[1] Or steel plate walls (SPWs).

https://doi.org/10.1016/j.acme.2018.06.012
1644-9665/

load was applied by diagonal corners via a 250 kN hydraulic jack. The panels were 300 mm deep, 300–450 mm wide and panel thickness was between 0.83 and 1.23 mm. Yield stresses of plates was considered equal to 219 and 152 MPa. Circular openings with 60, 105 and 150 mm diameters were tested at the center of plate. According to results, panel strength and stiffness are decreased due to the opening as follows [1].

$$\frac{V_{y\,Perf}}{V_{y\,Panel}} = \frac{K_{Perf}}{K_{Panel}} = \left(1 - \frac{D}{L}\right) \quad (1)$$

where D is the opening diameter, L is the panel width, $V_{y\ Perf}/V_{y\ Panel}$ and K_{Perf}/K_{Panel} are ratios of strength and stiffness of panel with opening to the corresponding specimen without opening. They also stated that the suggested relation had the highest reducing effect for the opening at the plate center. Therefore, the use of Eq. (1) is very conservative for other opening locations. They also stated that D parameter for the square and rectangular openings in Eq. (1) will be equal to diameter of circumscribed circle of the aforementioned openings [1,2]. They studied the strength and stiffness degradation of shear panel due to existence of a rectangular opening in stiffened and unstiffened panels and stated that strength and stiffness degradation due to the effect of opening are varied in panels with and without stiffener [3]. They also studied experimentally shear strength and stiffness of stiffened shear walls by making two symmetrical rectangular openings towards the plate center [4].

Bruneau and Purba modified Eq. (1) in perforated steel shear walls inside moment frame with reduced beam sections under a pattern of multiple regularly spaced circular openings throughout the infill plate using finite element method and numerical studies [5,6].

Alinia and Dastfan studied the effect of boundary members' rigidity on elastic shear buckling and post-buckling behavior of the panel via finite element method. As a result, torsional stiffness of boundary members had direct effect on increasing elastic buckling load but it was not effective on post-buckling strength. They also studied cyclic behavior, deformability and rigidity of stiffened SPSW [7–9]. Hosseinzadeh and Tehranizadeh studied via finite element methods the effect of great rectangular openings stiffened with local boundary elements on ductility, stiffness and shear strength of SPSW [10]. Valizadeh et al. studied experimentally the effect of opening sizes and slenderness ratio of steel plate on seismic behavior of steel plate shear walls under cyclic loads. Then, they studied amount of energy absorption of panels with openings using hysteresis curves resulted from specimens under study [11]. Similar experimental studies were conducted to investigate seismic behavior of stiffened and unstiffened shear walls with and without opening by Astaneh-Asl and the results were expressed in form of design codes based on seismic performance of steel shear walls [12]. Shekastehband et al. experimentally and numerically investigated the seismic behavior of high and low yield strength SPSWs with different circular opening ratios [13]. Sahebjam and Showkati experimentally studied the cyclic behavior of perforated carbon fiber reinforced polymer–steel composite shear walls in 2016 [14].

Seismic design of steel plate shear walls is based on very small thicknesses (in a fraction of mm) in upper floors of the building. Preparing such thin steel plates may be impossible in terms of availability. On the other hand, use of thicker plates increases shear capacity of the plate and subsequently ultimate load transferred to surrounding members. Thereupon, the demand for greater sections of adjacent beams and columns is increased. The simplest solution is to use a plate thicker than design demand and creation of opening for decreasing its stiffness. The present paper focuses on the effect of opening on decrease of shear strength of steel plate shear walls. As mentioned, theoretic relations are only valid for opening in the center of plate and their use for other areas

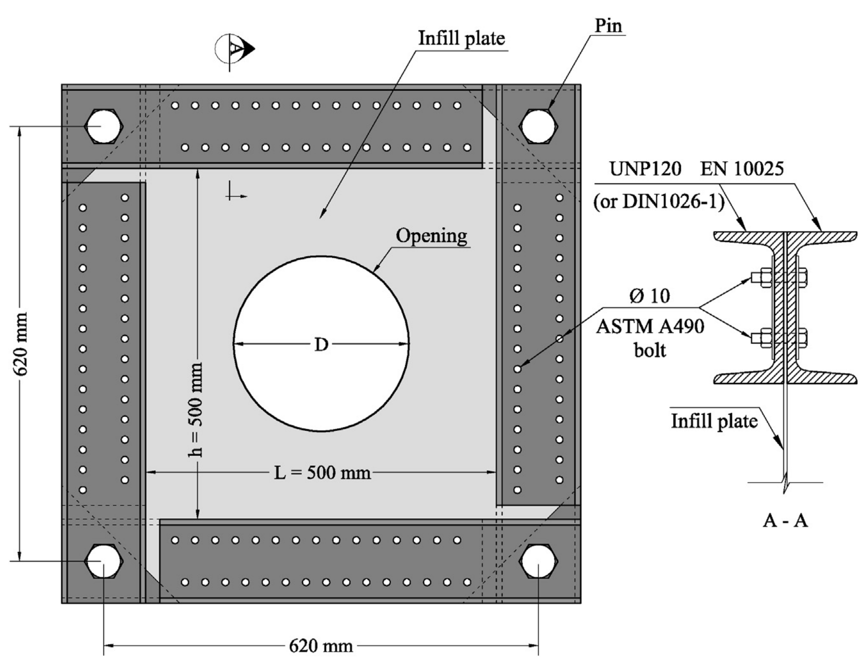

Fig. 1 – Geometric specifications of experimental specimens.

of the plate would be very conservative. Therefore, the current paper aims to present a simple relation for exact estimation of shear strength decrease of the wall with opening in any arbitrary location of the plate via finite element method.

2. Validation of modeling and mesh sensitivity

To reach the goal, numerous finite element models should be simulated and it is inevitable to verify the accuracy of finite element modeling and error calibrations at the beginning of calculations. Two experimental specimens of SPW2 and SPW8 of Valizadeh [11] were selected for mesh sensitivity analysis and validation based on their similarity with models of the present paper. In these two models, boundary members do not resist lateral loads due to simple connections and all loads are applied on the plate which is the main goal of present paper. Geometric specifications and material strength properties used in experimental specimens have been shown in Fig. 1 and Table 1, respectively.

Cyclic loading of experimental specimens and application of drift from 0.5% in linear range to maximum 6% in nonlinear range with low speed were done to avoid dynamic modes. Time history of displacement applied on specimens is based on Fig. 2.

Above experimental models have simple surrounding hinge frame. In this respect, beam to column connection is simple in finite element method and it has been simulated by triangulation of beam web at the column flange junction. Such method has been used to simulate simple connection of column base to deep beam as well (Fig. 3b). 4-Node shell element (SHELL181) was used in ANSYS [15] to simulate the plate and surrounding frame. To validate the modeling, finite element simulation of SPW2 specimen was done according to Fig. 3(a) and cyclic loading was applied on the model. Results of the finite element modeling have been shown in Fig. 3(b).

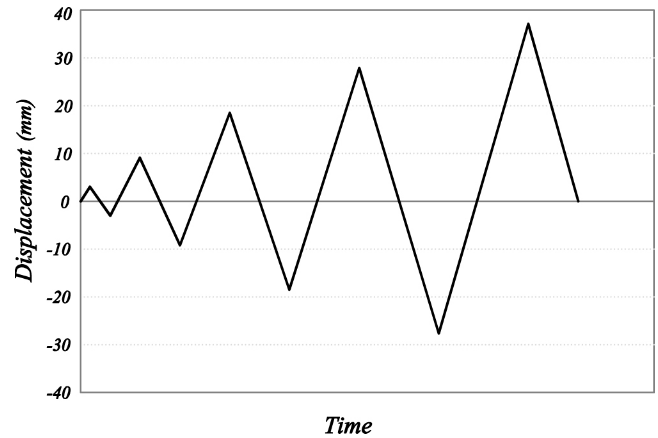

Fig. 2 – Time history of displacement applied on specimens.

The comparison of results obtained from analysis of finite element model and experimental specimen shows proper match of modeling with experimental results as shown in Fig. 4. As can be seen in figure, there is a tangible difference of elastic stiffness between finite element model and experimental specimen. It is noteworthy that infill plate connections to boundary members are not modeled in finite element analysis which leads to higher model stiffness than experimental specimen. In some experimental specimens of Valizadeh et al. [11], bearing failure of the model was due to fracture in connections of plates and bolts, while the cyclic behavior of finite element model continued due to lack of yield of connection elements and showed higher stiffness than experimental test. Complete adaptation of elastic stiffness of analytical model with expected stiffness of the theoretical relations proves the above-mentioned materials.

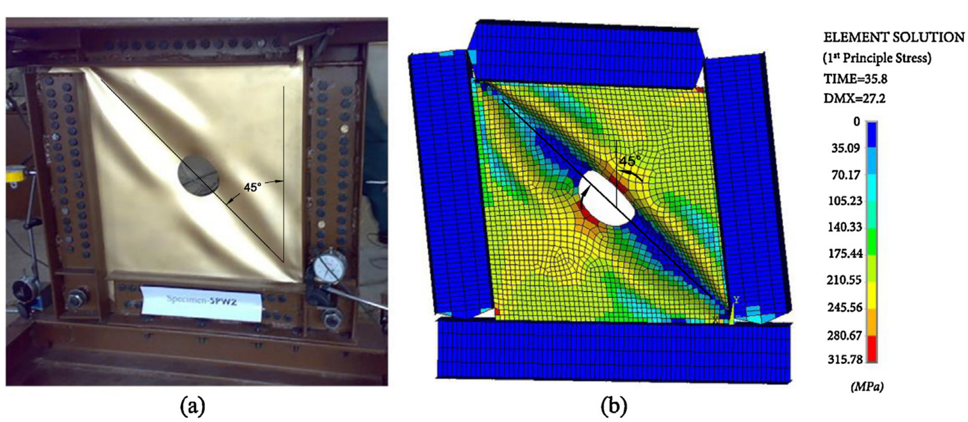

Fig. 3 – Results of (a) experimental specimen SPW2 [11], (b) finite element model.

Table 1 – Strength and geometric specifications of infill plates.

Experimental specimen	Material type	Plate thickness (mm)	Opening diameter (mm)	Yield stress (MPa)	Ultimate stress (MPa)
SPW2	EN 10025-S185	0.7	100	180	300
SPW8	EN 10025-S275	0.37	250	299	375

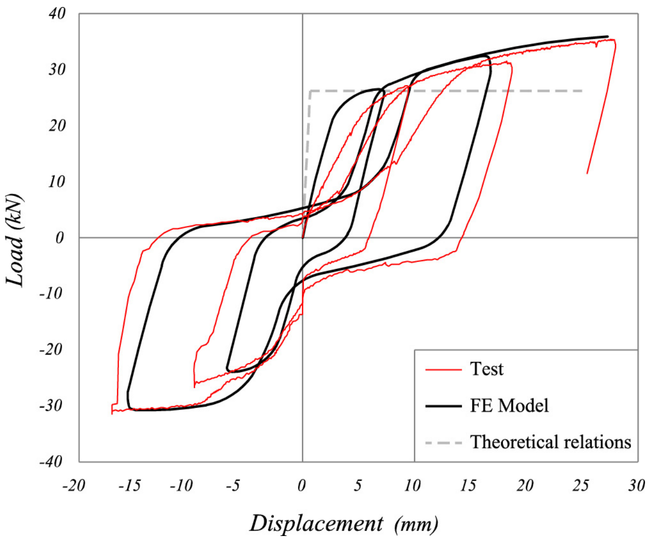

Fig. 4 – Hysteresis curve of finite element model and specimen SPW2.

To do mesh sensitivity analysis, different mesh sizes have been considered (Fig. 5) and monotonic lateral load was applied on the second model (SPW8). Comparison of results of finite element model and push over curve of experimental specimen has been shown in Fig. 5. It suggests proper match of the model with experimental results. Results indicate that if the maximum mesh sizes are smaller than 15 mm, calculational accuracy is not increased but time of analysis is increased greatly. For example, for any certain lateral displacement, the maximum difference between load carrying capacity of push over curves with 10- and 15-mm mesh sizes is less than 2.04% (Fig. 5). While analytical time of the model with 10-mm mesh was 3.5 times higher than the model with 15-mm mesh size.

15-mm mesh that matches properly with experimental results has been chosen for meshing steel plate shear wall. Then, 75- and 150-mm mesh sizes were used based on aspect ratio of infill plate and its dimensional proportionality with the verification model under study.

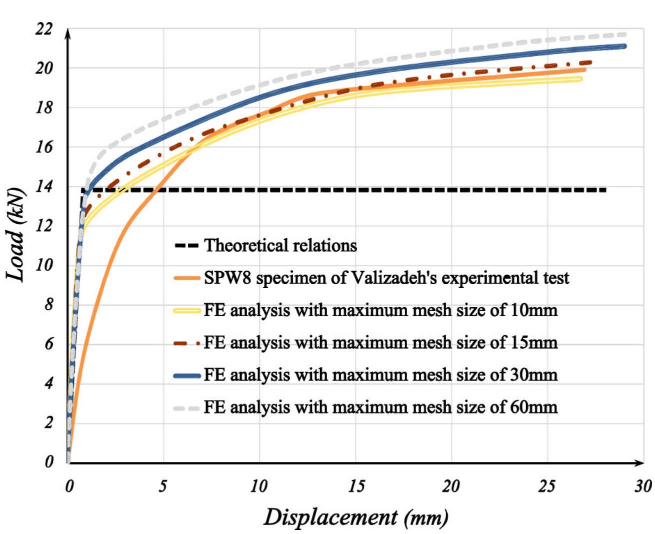

Fig. 5 – Mesh sensitivity analysis.

3. Modelling specimens under study

Since the present research aims to study the shear strength degradation of the shear wall due to existence of opening in different location of the plate compared to strength of specimen without opening, it is necessary to model correctly the panel without opening and to control the accuracy of the shear strength with the amounts obtained from theoretic relations. Given common bay length in buildings, a steel shear wall with 5 m wide, 3 m high and 2.5 mm thick has been considered with a simple connection surrounding frame. Stiffness of beam and column is such that the plate is completely under pure shear. To select proper sections for surrounding beam and columns with sufficient rigidity, the specifications of AISC341-10 [16] were used. Preliminary design of surrounding vertical elements and the connecting horizontal element due to its simple connections to adjacent columns have been carried out by the use of Eqs. (2) and (3), respectively [16].

$$I_c \geq 0.0031\left(\frac{t_w h^4}{L}\right) \tag{2}$$

$$M_{pb} > \frac{(\sigma_{ty} t_w L^2 \cos^2\alpha)}{8} \tag{3}$$

where I_c, t_w, h, L and M_{pb} are column moment of inertia, plate thickness, plate height, plate width and plastic moment capacity of beam, respectively. α is the diagonal tension field angle as shown in Eq. (4) [16] and the stress of tension field in yielding time (σ_{ty}) is obtained by solving Eq. (5) [2].

$$\tan^4\alpha = \frac{\left(1+\frac{t_w L}{2A_c}\right)}{\left[1+t_w h\left(\frac{1}{A_b}+\frac{h^3}{360 I_c L}\right)\right]} \tag{4}$$

$$\sigma_{ty}^2 + 3\tau_{cr}\sigma_{ty}\sin(2\alpha) + 3\tau_{cr}^2 - f_y^2 = 0 \tag{5}$$

In above equations, A_c, A_b and τ_{cr} are column cross sectional area, beam cross sectional area and the critical buckling shear stress of steel plate, respectively. τ_{cr} can be determined in accordance with classical stability equation [17] as follows:

$$\tau_{cr} = \frac{k\pi^2 E}{12(1-\nu^2)}\cdot\left(\frac{t_w}{L}\right)^2 \leq \tau_y = \frac{f_y}{\sqrt{3}} \tag{6}$$

in which ν, E, τ_y and f_y are Poisson's ratio (0.3), elasticity modulus, shear yielding stress and uniaxial tensile yielding stress of the plate, respectively. The shear buckling factor k which depends on the steel plate aspect ratio and boundary conditions, is equal to 18.861 for the simple supported plate of the present study. As a result, for the wall with mentioned sizes, beams and columns of type IPB300 were designed and modeled as shown in Fig. 6.

ST37 with modulus of elasticity of 205.94 GPa and yield stress of 235.36 MPa was used in all members with ideal

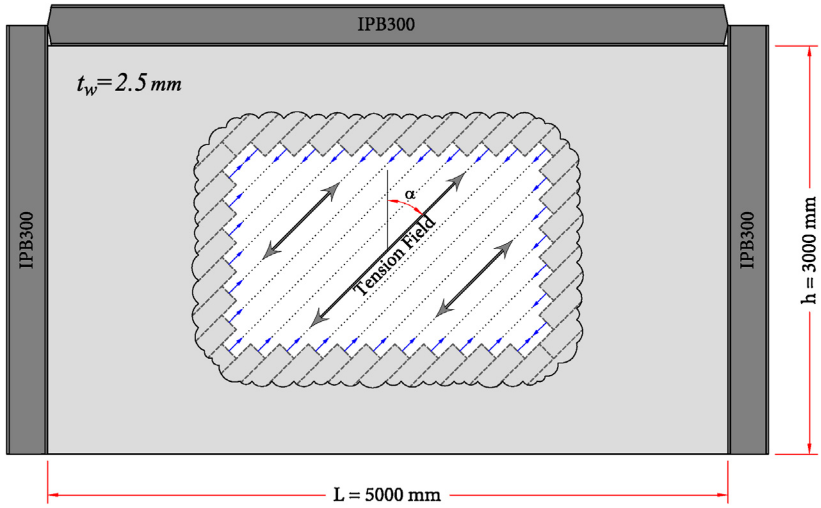

Fig. 6 – Dimensions and specifications of shear panel without opening.

bilinear stress-strain curve without hardening (elastic-perfectly plastic). Since removal of bottom beam will reduce time of analyses, bottom beam is removed in all simulations and simple boundary condition is applied on column base and wall directly. According to theoretic relations based on classical stability equation [16,17] and also considering the insignificant value of τ_{cr} (0.878 MPa $\approx$ 0) obtained from Eq. (6), σ_{ty} is almost equal to specified minimum yield stress (uniaxial yield stress, f_y) of infill plate, and hence shear strength of steel plate shear wall is calculated as follows [16].

$$V_y = 0.5\, f_y L t_w \sin(2\alpha) \tag{7}$$

Concerning the value of α (42.7°) which was obtained by Eq. (4), theoretical shear strength of the wall is 1467.08 kN. Based on finite element model analysis of unstiffened panel, shear strength of the plate is 1427.85 kN that shows 2.7% error compared to analytical amount of 1467.08 kN. This demonstrates the proper accuracy of mesh sizes and modeling process.

3.1. *Introducing models based on the arrangement of opening*

To study behavior of panels with opening, 15 models with 0.8 m opening's diameter were considered for push over analysis as shown in Fig. 7.

An initial imperfection between 0.03 and 0.05 mm was applied to each model in order to gain convergence of the nonlinear pushover analysis results.

4. Analysis and study of results

4.1. *Analysis of force–displacement curves of models*

As shown in Fig. 8, results of finite element analysis of 15 models show that the closer the location of opening to formation of diagonal tension field of the plate, the higher the strength degradation of the specimen. For this reason, the model $SPSW_{(L/h\,=\,1.67)}8$ which is exactly at the center of the plate (start of formation of diagonal tension field due to maximum shear stresses) has the lowest shear strength and the model $SPSW_{(L/h\,=\,1.67)}1$ located at the farthest zone from diagonal tension field has the highest strength. Therefore, no significant difference can be seen between strength of specimen 1 and the model without opening. In other words, by distance of the opening from the center of plate either horizontally or vertically, strength degradation of models will be small due to reduction of opening involvement in formation of diagonal tension field. Out of plane deformation of specimens resulted from push over analysis on all specimens has been shown in Fig. 9.

Another significant point in study of opening position is tangible change of diagonal tension field angle. Fig. 10 shows the distribution of the first principle stress in infill plate of some specimens to see objectively the change of diagonal tension field angle.

As seen in Fig. 10, in models $SPSW_{(L/h\,=\,1.67)}1$ and 15, The angle is very close to diagonal tension field angle of the specimen without opening whereas in models $SPSW_{(L/h\,=\,1.67)}5$, 9 and 11, The angle fractured and had two different values on both sides of the opening ($\alpha \neq \beta$). Change of diagonal tension field angle around the opening is because the plate is divided into sub panels due to existence of the opening and formation of diagonal tension field in any sub panel will be based on Eq. (4) regarding stiffness of surrounding members of the same panel.

4.2. *Determining semi-empirical relation for estimation of specimen's strength*

We require defining yield point of the model to determine a semi-empirical relation which suggests strength degradation of models compared to those without opening. In present research, according to plastic energy equilibrium [18], idealized bilinear force–displacement curve is replaced by the real push over curve of the model given elastic-perfectly plastic

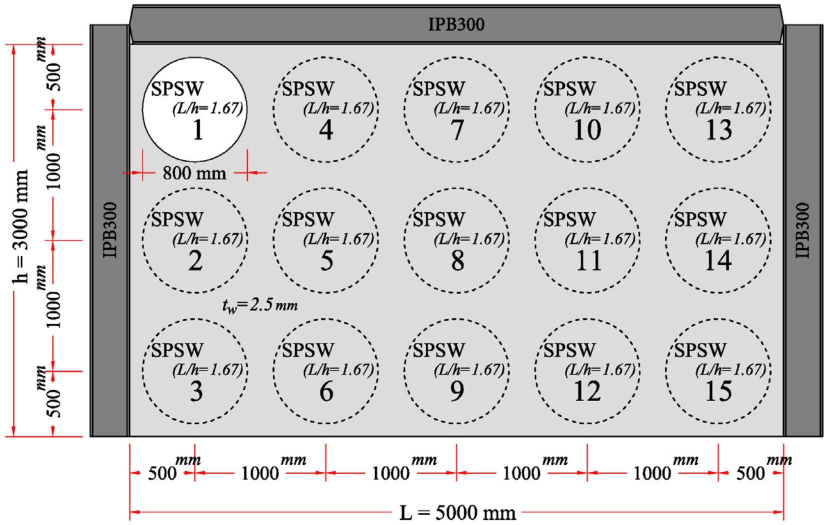

Fig. 7 – Nomenclature of selected models to study panel shear strength.

behavior (without hardening or softening) after yielding. For this purpose, the point B (as shown in Fig. 11) should be chosen by using an iterative graphical procedure in such a way that the areas enclosed by the idealized bilinear curve and nonlinear push over curve are balanced below and above the idealized bilinear curve.

Where V_y, V_u, K_e, δ_y and δ_u are effective shear yield strength (shear strength), ultimate lateral load carrying capacity of shear panel, effective shear stiffness, limiting elastic shear displacement and displacement in ultimate load carrying capacity, respectively. The amounts of effective shear yield strength of specimens obtained by equivalent bilinear force–displacement curve and percent of strength degradation of each specimen have been shown in Table 2.

Concerning results of Table 2, the semi-empirical relation, defining the percent of decrease of shear strength in specimens with opening compared to specimens without opening, can be determined. Therefore, the amounts of shear strength of models shown in Table 2 are plotted firstly on a graph. Thence, the best passing surface through mentioned strengths has been fitted via trial and error using MATLAB [19] software (Fig. 12).

The equation of this surface presents absolute value of shear strengths of each panel based on opening coordinates in steel plate shear wall. But the desired goal of the present paper (proposing a relation that suggests the percent of decrease of shear strength in models with arbitrary opening location by the use of dimensionless parameters of opening coordinates)

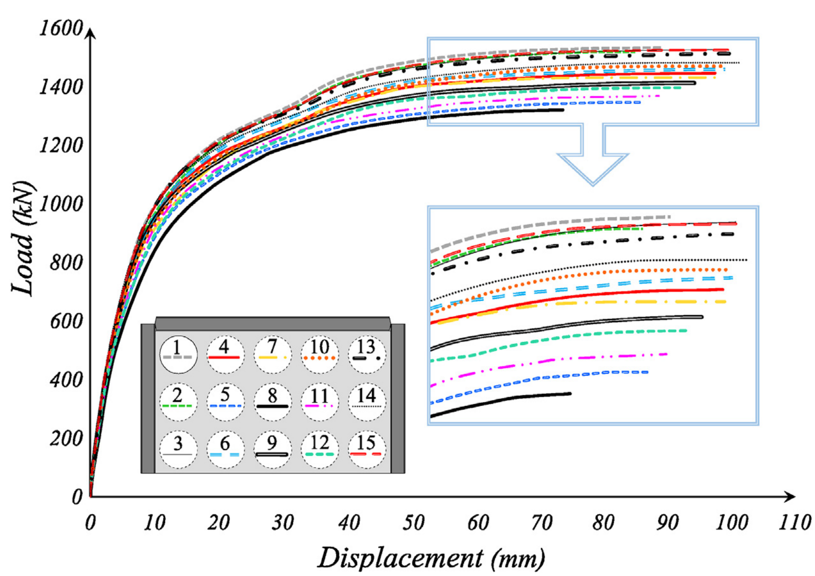

Fig. 8 – Push over curves of panels due to opening displacement.

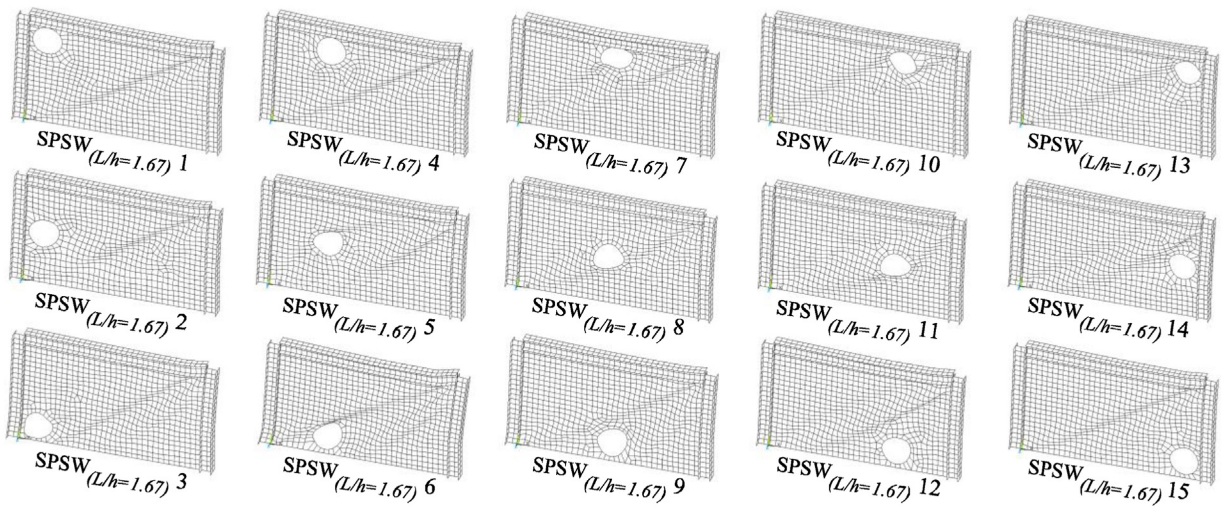

Fig. 9 – Out of plane buckling and involvement of opening in specimen's deformation.

is achieved by inverting the obtained surface using natural coordinate system and satisfaction of boundary condition. For this purpose, new coordinate system of ξ and η shown in Fig. 13 is defined at the center of plate in form of Eqs. (8) and (9).

$$\xi = \frac{2x}{L} \quad (8)$$

$$\eta = \frac{2y}{h} \quad (9)$$

In above relations, x and y towards natural coordinate of the plate center vary between $-L/2$ and $L/2$ and between $-h/2$ and $h/2$ respectively. Thus ξ and η will have amounts between -1 and 1.

Considering the highest strength degradation (D/L) in Eq. (1) for placement of opening at the center of the plate or in the center of defined coordinate ($\xi = \eta = 0$), the final relation is obtained as Eq. (10) which shows percent of decrease of shear strength in specimens with opening compared to those without opening.

$$\Delta Vy = (1-\xi^2)(1-\eta^2)\left(\frac{D}{L}\right) \times 100 \quad (10)$$

The amounts related to percent of strength degradation of 15 specimens under study have been shown in Table 3 using relation (10) and based on dimensionless coordinate of openings (ξ and η). By having geometric specifications of the opening (equivalent circular opening diameter), opening coordinate and without the need for carrying out the finite

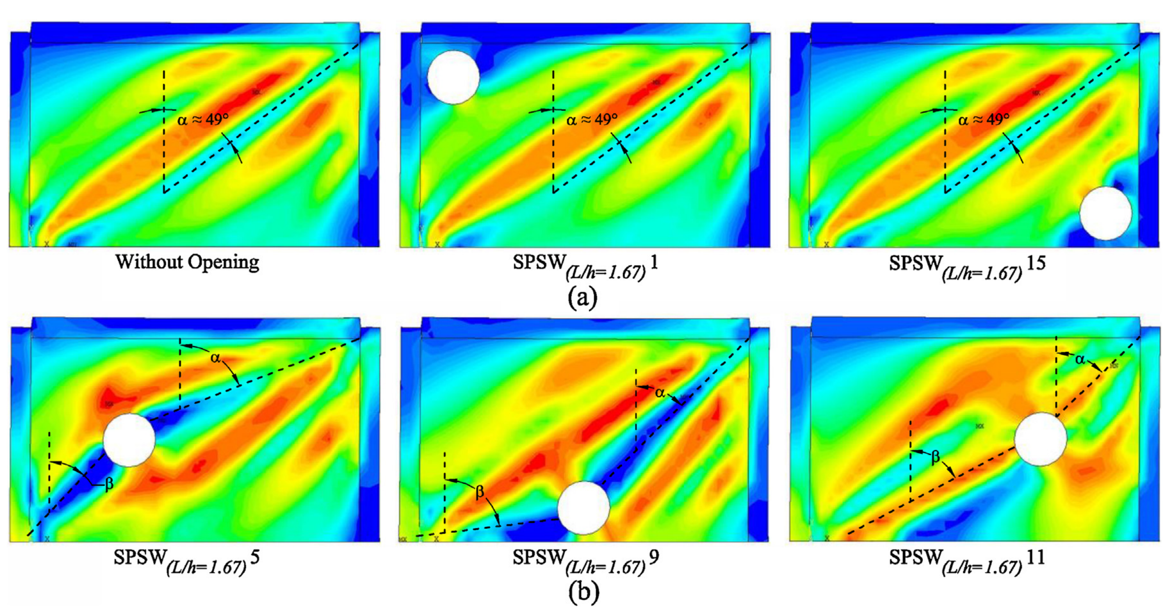

Fig. 10 – Distribution of the first principle stress for (a) specimens without change of angle α and (b) specimens with fracture of angle α.

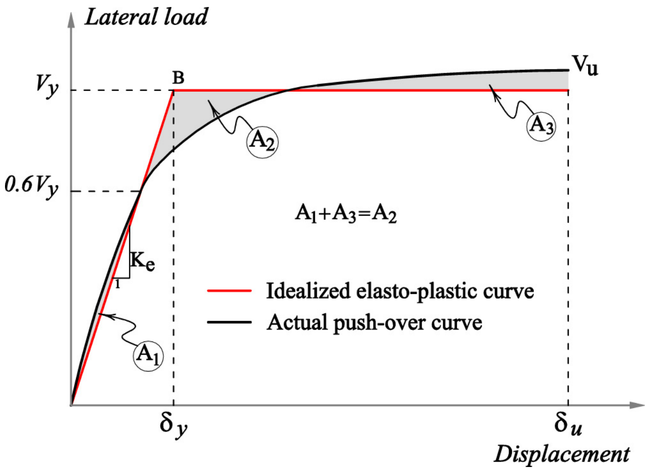

Fig. 11 – Behavioral model selected for determination of the yield point.

element analysis, the suggested relation is able to estimate the percent of strength degradation of the panel in any location of the plate which is one of the main advantages of the present paper.

Comparison of percent of strength degradation of the models based on suggested relation (10) (the fourth column of Table 3) and corresponding amounts of finite element analysis (the third column of Table 2) shows proper match of the amounts and accuracy of the suggested relation (10). It is noteworthy that the results of estimating the strength degradation percent using the proposed relationship (10) and FEM should not differ by more than 5%. For example, percent of strength degradation of the model $SPSW_{(L/h\,=\,1.67)}5$ resulted from finite element analysis is equal to 12.71%. This amount is obtained as 13.44% by using $\xi = (-1/2.5) = -0.4$ and $\eta = 0$ and substituting in suggested relation (10). The difference between two aforementioned values is 0.73%, which is less than 5%. The maximum absolute value of the difference between the two methods is 3.36% for rectangular panels. This is the reason of authors' positive evaluation of the proposed relationship.

Table 2 – Shear yield strength and strength degradation percentage of specimens under study.

Model	Vy (kN)	$\Delta Vy_{\text{Finite Element}}$ (%)
$SPSW_{(L/h\,=\,1.67)}1$	1422.95	0.34
$SPSW_{(L/h\,=\,1.67)}2$	1393.53	2.40
$SPSW_{(L/h\,=\,1.67)}3$	1420.01	0.55
$SPSW_{(L/h\,=\,1.67)}4$	1344.50	5.84
$SPSW_{(L/h\,=\,1.67)}5$	1246.43	12.71
$SPSW_{(L/h\,=\,1.67)}6$	1352.34	5.29
$SPSW_{(L/h\,=\,1.67)}7$	1339.59	6.18
$SPSW_{(L/h\,=\,1.67)}8$	1226.82	14.08
$SPSW_{(L/h\,=\,1.67)}9$	1328.81	6.94
$SPSW_{(L/h\,=\,1.67)}10$	1362.15	4.6
$SPSW_{(L/h\,=\,1.67)}11$	1262.12	11.61
$SPSW_{(L/h\,=\,1.67)}12$	1308.21	8.38
$SPSW_{(L/h\,=\,1.67)}13$	1411.18	1.17
$SPSW_{(L/h\,=\,1.67)}14$	1384.71	3.02
$SPSW_{(L/h\,=\,1.67)}15$	1409.22	1.30

It should be noted that effective shear yield strength of all specimens in finite element analysis was obtained by nonlinear static analysis (push over) of specimens under monotonic loading. It means that if loading is applied in opposite direction or cyclic loading of specimens is mentioned, it can be expected that specimens with symmetrical opening (for example, the models $SPSW_{(L/h\,=\,1.67)}1$ and $SPSW_{(L/h\,=\,1.67)}13$) have the same behavior in strength degradation. Interestingly, this is true about amounts estimated by suggested relation (10).

From this point of view, it can be concluded that performance of proposed equation has been even more successful than finite element monotonic push over in estimating the real strength degradation of specimens in case of the acceptance of validity of proposed relation. In other words, suggested relation has been able to estimate the real strength degradation to some extent better than finite element push over method according to the central symmetry aspect of opening locations (Fig. 14). This is the second advantage of present paper compared to finite element analysis.

As seen in Fig. 14, specimens with symmetrical openings towards the center of the plate have the same strength degradation due to application of suggested relation (10). Another significant point in Fig. 14 is complete conformity of strength degradation resulted from relation (10) for specimen with opening in the plate center ($SPSW_{(L/h\,=\,1.67)}8$) and corresponding amount resulted from theoretical Eq. (1).

As mentioned in the introduction, theoretical Eq. (1) is only valid for opening at the plate center and its use for all other locations of openings is conservative as shown in Fig. 14. Accordingly, use of Eq. (1) for estimation of strength degradation of specimens such as $SPSW_{(L/h\,=\,1.67)}1$, will be followed by the highest relative error (12.8%). This will show advantageous use of suggested relation as well as finite element method in estimating the strength degradation of the specimen with opening in the areas other than the plate center compared to theoretical relations.

5. Verification of proposed relation

In order to validate the proposed relationship several models have been considered with various conditions of wall geometry, plate thicknesses and opening shape. This verification is to examine the effect of the change in each of the variables reflected in the proposed relationship. In Section 5.1 the accuracy of the proposed relationship is only measured by the change effect of opening location, so that the only difference between the verification model and the models generating the proposed relationship be in the opening location. The effect of simultaneous change of the opening location, the opening dimensions and diameter are measured in Sections 5.2 and 5.3. Finally, the proposed relationship accuracy is controlled for changes in the opening shape in Section 5.4. In all of the abovementioned cases, it has been tried to measure the efficiency of the proposed relationship for different thicknesses by changing the plate thickness of the verification models compared to the plate thickness used in the generating models of proposed relationship.

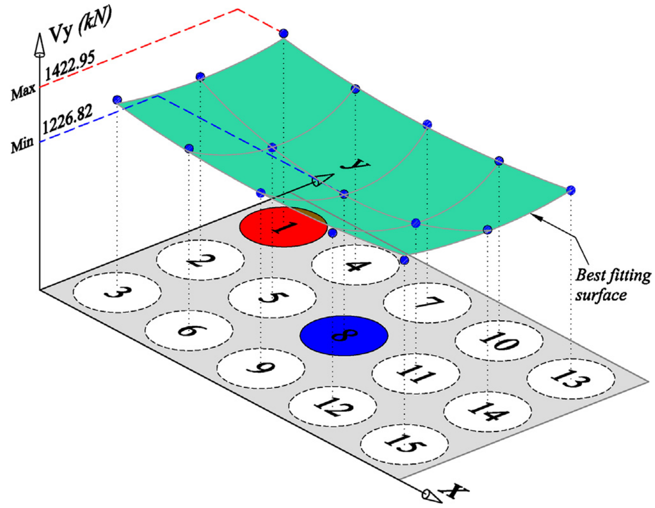

Fig. 12 – Fitness of the best surface passing through shear strengths of models.

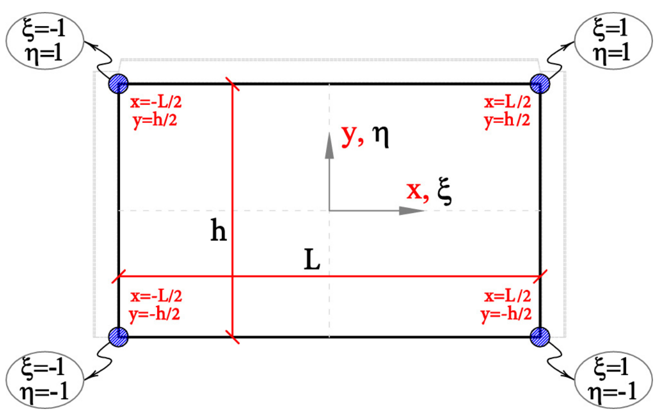

Fig. 13 – Coordinate system defined for extraction of ξ and η.

5.1. *Shear panels with width to height ratio of 1.67*

To control accuracy of relation (10), simulation of a new model, so called Test$_{(L/h\,=\,1.67)}$1, with all the same geometric specifications (opening diameter, plate thickness, width to height ratio and surrounding members) of the previous models has been done in such a way that the only difference of the mentioned model with other 15 models producing the relation (10), is the location of the opening. After pushover of the specimen and calculation of percent of strength degradation compared to the specimen without the opening and also comparing the obtained value with corresponding amount obtained from relation (10), performance accuracy of interpolation functionality of suggested function is measured. The opening coordinate of the specimen was selected as $x = -1.5$ m and

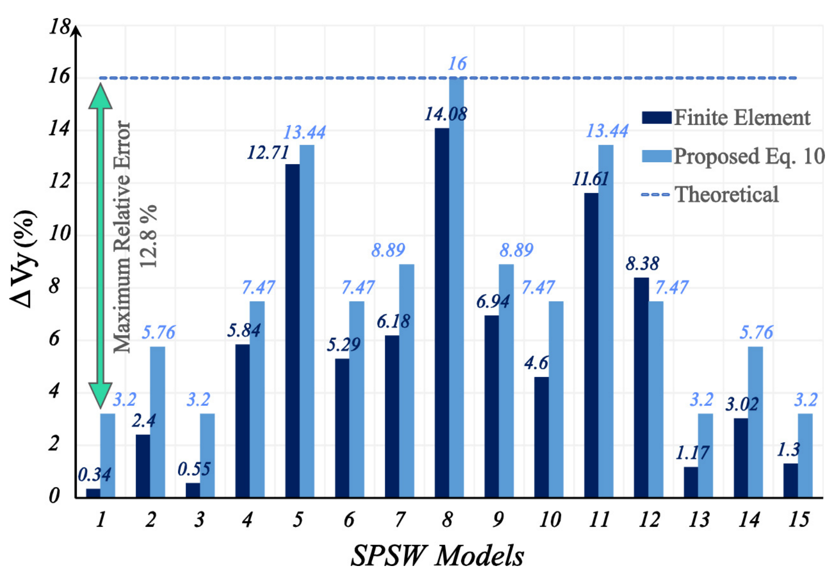

Fig. 14 – Comparing strength degradation resulted from suggested relation and finite element.

Table 3 – Strength degradation percent of specimens compared to model without opening based on proposed equation.

Model	ξ	η	$\Delta Vy_{\text{Proposed Eq. (10)}}$ (%)
$SPSW_{(L/h=1.67)}1$	−0.8	0.667	3.20
$SPSW_{(L/h=1.67)}2$	−0.8	0.0	5.76
$SPSW_{(L/h=1.67)}3$	−0.8	−0.667	3.20
$SPSW_{(L/h=1.67)}4$	−0.4	0.667	7.47
$SPSW_{(L/h=1.67)}5$	−0.4	0.0	13.44
$SPSW_{(L/h=1.67)}6$	−0.4	−0.667	7.47
$SPSW_{(L/h=1.67)}7$	0.0	0.667	8.89
$SPSW_{(L/h=1.67)}8$	0.0	0.0	16.00
$SPSW_{(L/h=1.67)}9$	0.0	−0.667	8.89
$SPSW_{(L/h=1.67)}10$	0.4	0.667	7.47
$SPSW_{(L/h=1.67)}11$	0.4	0.0	13.44
$SPSW_{(L/h=1.67)}12$	0.4	−0.667	7.47
$SPSW_{(L/h=1.67)}13$	0.8	0.667	3.20
$SPSW_{(L/h=1.67)}14$	0.8	0.0	5.76
$SPSW_{(L/h=1.67)}15$	0.8	−0.667	3.20

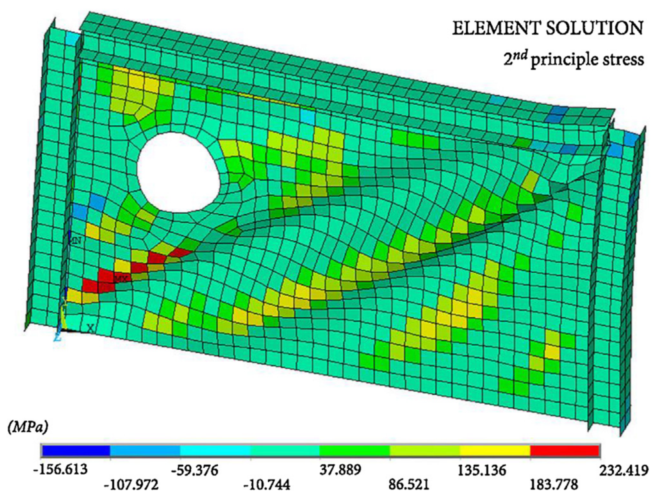

Fig. 15 – Distribution of the second principle stress in the specimen $Test_{(L/h=1.67)}1$.

y = 0.45 m by placement of coordinate origin at the plate center and the specimen was subject to loading (Fig. 15).

The effective shear yield strength of the specimen resulted from push over analysis is equal to 1303.7 kN as shown in Fig. 16. This value is 8.7% lower than the specimen without opening. Percent of strength degradation of the model $Test_{(L/h=1.67)}1$ with $\xi = (-1.5/2.5) = -0.6$ and $\eta = (0.45/1.5) = 0.3$ and substitution of it in relation (10) is 9.32% suggesting proper accuracy of relation (10) in estimation of percent of decrease of shear strength.

5.2. *Shear panels with width to height ratio of 1*

To verify the suggested relation (10) for square shear panels with width to height ratio of 1, 9 square specimens with 3 m wide and high were known as $Test_{(L/h=1.0)}1$ to $Test_{(L/h=1.0)}9$. The opening position of all 9 specimens and the models' nomenclature have been shown in Fig. 17. By selecting 0.9 m openings diameter, panels with 3 m wide and 9 different locations of openings, the

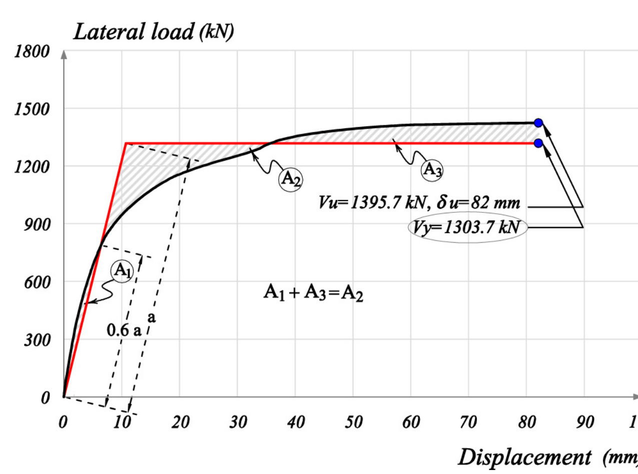

Fig. 16 – Shear yield strength of specimen $Test_{(L/h=1.67)}1$ with idealized bilinear curve.

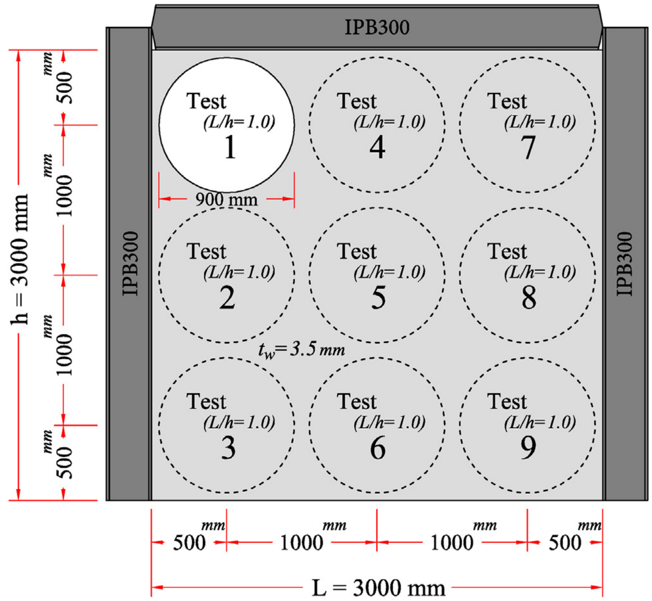

Fig. 17 – New models for controlling the accuracy of relation 10 for square panel.

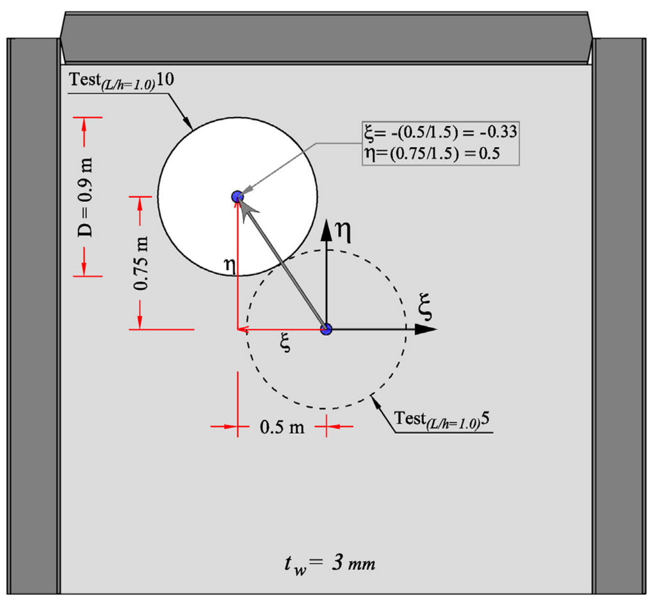

Fig. 18 – Geometric specifications of Test$_{(L/h\,=\,1.0)}$10.

Table 4 – Percent of strength degradation of specimens under 2 evaluated modes.

Model	$Vy_{\text{Finite Element}}$ (kN)	$\Delta Vy_{\text{Finite Element}}$ (%)	$\Delta Vy_{\text{Proposed Eq. (10)}}$ (%)
Test$_{(L/h\,=\,1.0)}$1	1102.51	8.0	9.26
Test$_{(L/h\,=\,1.0)}$2	982.67	18.0	16.67
Test$_{(L/h\,=\,1.0)}$3	1078.54	10.0	9.26
Test$_{(L/h\,=\,1.0)}$4	989.50	17.43	16.67
Test$_{(L/h\,=\,1.0)}$5	855.64	28.6	30
Test$_{(L/h\,=\,1.0)}$6	1023.42	14.60	16.67
Test$_{(L/h\,=\,1.0)}$7	1088.13	9.2	9.26
Test$_{(L/h\,=\,1.0)}$8	994.42	17.02	16.67
Test$_{(L/h\,=\,1.0)}$9	1072.55	10.5	9.26

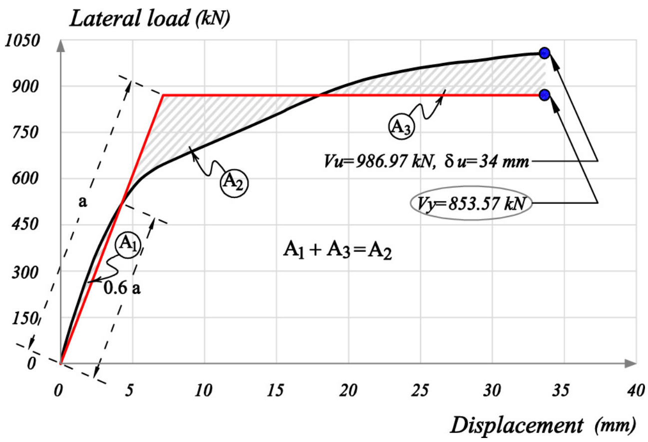

Fig. 19 – Shear yield strength of Test$_{(L/h\ =\ 1.0)}$10 with idealized bilinear curve.

effect of change in all variables of the proposed relation was studied. Concerning absence of thickness parameter of steel plate in suggested relation, plate thickness of specimens is different from previous models and it is 3.5 mm thus the accuracy of the relation is confirmed for all plate thicknesses as well as its independency on the plate thickness. Analytical result of square panel without opening was 1198.38 kN which was less than 1.5% different from the expected amount obtained by theoretical relations (1216.03 kN) and it is acceptable as simulation error.

Results of analysis in terms of the percent of decrease of shear strength of specimens with opening compared to those without opening have been shown in Table 4 under relation (10) and finite element method.

Comparing corresponding amounts in Table 4, it is seen that relation (10) can estimate strength degradation of square panels even more accurate than rectangular panels with width to height ratio of over 1. The maximum difference between output of relation (10) and that of finite element method for estimation of percent of effective shear yield strength degradation was 3.36 and 2.07% for rectangular and

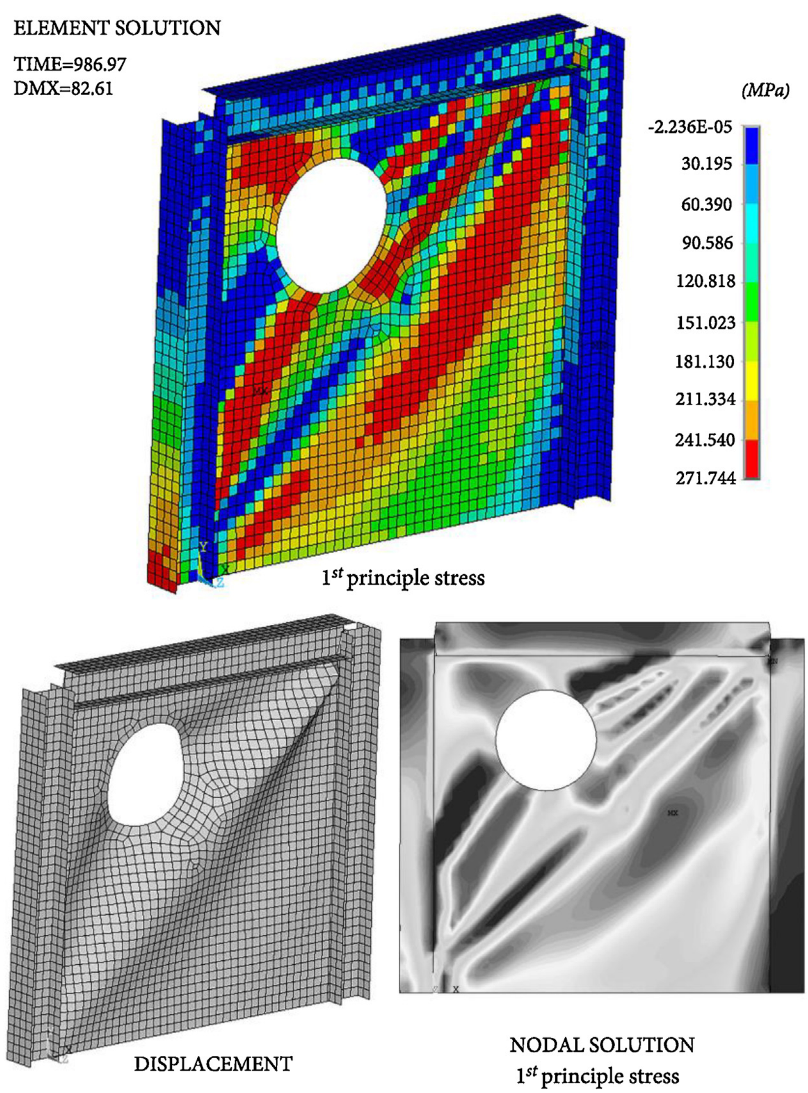

Fig. 20 – Distribution of the first principle stress and deformation of the model.

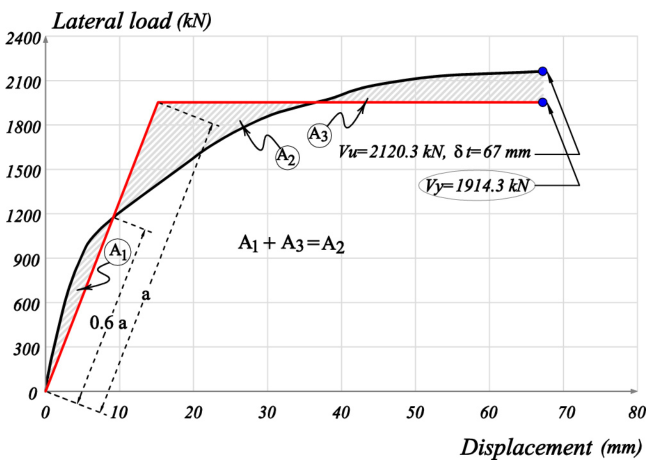

Fig. 21 – Shear yield strength of Test$_{(L/h\,=\,2.0)}$1 with idealized bilinear curve.

square panels, respectively. This shows proper accuracy of relation (10) for estimating the shear strength degradation percentage.

For final control of relation (10) for opening positions other than those included in Fig. 17, a new model with a 0.9 m diameter opening in coordinates of $x = -0.5$ m, $y = 0.75$ m and a plate thickness of 3 mm was selected and loaded as shown in Fig. 18.

The aforementioned model name is Test$_{(L/h\,=\,1.0)}$10. Effective shear yield strength of the model resulted from push over analysis is 853.57 kN as shown in Fig. 19. This amount is 18.34% lower than strength of the specimen without opening (1045.23 kN).

Substituting $\xi = (-0.5/1.5) = -0.33$ and $\eta = (0.75/1.5) = 0.5$ in relation (10), percent of strength degradation of the specimen is equal to 20% which suggests proper accuracy of relation (10) in estimation of percent of decrease of shear strength of square panels.

Out of plane displacement has been shown in Fig. 20 as well as distribution of the first principle stress at ultimate load carrying capacity.

5.3. *Panels with width to height ratio of 2*

The specimen Test$_{(L/h\,=\,2.0)}$1 aims to study the behavior of shear panel with 6 m wide, 3 m high and to control the validity of suggested relation (10) for width to height ratio of 2 in addition to 1 and 1.67 ratios. Concerning 3 mm plate thickness and 1 m opening diameter at $x = -2$ m and $y = 0$ m towards the plate center, 1914.27 kN was obtained for shear yield strength of the model via finite element push over analysis as shown in Fig. 21.

This model has 9.46% strength degradation compared to the model without opening. The degradation amount was calculated as 9.26% using relation (10) suggesting accuracy of relation (10). Results of finite element analysis of the model have been shown in Fig. 22 regarding stress state ratio of plate. The figure shows clearly the state of elements affected by diagonal tension filed of the model.

5.4. *Openings with square and rectangular shapes*

As seen in research history of the paper, D parameter in Eq. (1) for square opening is equivalent to circumscribed circle diameter of the opening [1,2]. To study accuracy of relation (10) in terms of shape of the opening, Test$_{(L/h\,=\,2.0)}$2 with width to height ratio of 2, 6 m wide, 3 m high and 3 mm thick as well as square opening with 1.2 m long is selected as shown in Fig. 23. The position of square opening in Test$_{(L/h\,=\,2.0)}$2 was selected in symmetrical position of Test$_{(L/h\,=\,2.0)}$1 with circular opening.

All specifications of Test$_{(L/h\,=\,2.0)}$2 are similar to Test$_{(L/h\,=\,2.0)}$1 except for the shape of opening. The square opening with the dimension of 1.2 m long is equivalent to circular opening with 1.7 m diameter thus the difference of these two models is extra 1.7 m diameter [3]. According to the mentioned specifications, relation (10) estimates the strength degradation of Test$_{(L/h\,=\,2.0)}$2 as 15.74% compared to the specimen without opening.

The effective shear yield strength resulted from finite element analysis of the model is 1816.2 kN suggesting 14.1% strength degradation compared to the model without opening. 1.64% difference between results of finite element analysis and relation (10) shows accuracy of relation (10) for different shapes of openings. Fig. 24 indicates distribution of von Mises stress of the model's infill plate.

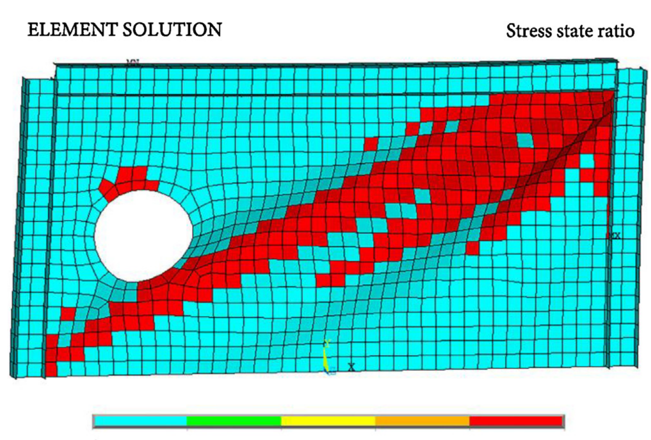

Fig. 22 – Stress state ratio and deformation of Test$_{(L/h\,=\,2.0)}$1.

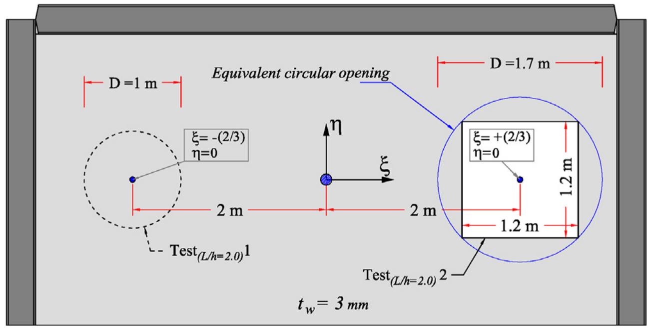

Fig. 23 – Geometry of Test$_{(L/h = 2.0)}$2.

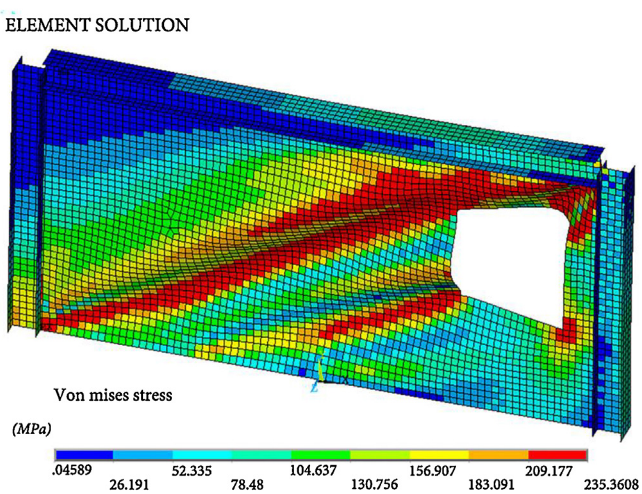

Fig. 24 – Distribution of von Mises stress and deformation of Test$_{(L/h = 2.0)}$2.

6. Conclusion

In the present paper, percent of decrease of shear strength of steel plate shear walls with arbitrary located opening was studied via finite element method. Results indicated that it was possible to reach simple relations to calculate accurately the amount of strength degradation in a panel with opening in any optional location compared to the panel without opening. As a result, the empirical and dimensionless relation (10) was presented in this regard. Results indicated that the proposed relation is appropriate for estimation of percent of strength degradation of shear panels with concentrated opening in any location of the plate and has been able to reduce the error for the models under study up to 16% compared to conservative use of conventional Eq. (1). Based on simulation results, use of proposed equation is valid for all rectangular panels with width to height ratio over 1 and square panels with any thicknesses.

REFERENCES

[1] T.M. Roberts, S. Sabouri-Ghomi, Hysteretic characteristics of unstiffened perforated steel plate shear panels, Thin-Walled Struct. 14 (1992) 139–151. , http://dx.doi.org/10.1016/0263-8231(92)90047-Z.

[2] T.M. Roberts, Seismic resistance of steel plate shear walls, Eng. Struct. 17 (1995) 344–351. , http://dx.doi.org/10.1016/0141-0296(95)00017-2.

[3] S. Sabouri-Ghomi, E. Ahouri, R. Sajadi, M. Alavi, A. Roufegarinejad, M.A. Bradford, Stiffness and strength degradation of steel shear walls having an arbitrarily-located opening, J. Constr. Steel Res. 79 (2012) 91–100. , http://dx.doi.org/10.1016/j.jcsr.2012.07.017.

[4] S. Sabouri-Ghomi, S. Mamazizi, Experimental investigation on stiffened steel plate shear walls with two rectangular openings, Thin-Walled Struct. 86 (2015) 56–66. , http://dx.doi.org/10.1016/j.tws.2014.10.005.

[5] R. Purba, M. Bruneau, Finite-element investigation and design recommendations for perforated steel plate shear walls, J. Struct. Eng. 135 (2009) 1367–1376. , http://dx.doi.org/10.1061/(ASCE)ST.1943-541X.0000061.

[6] D. Vian, M. Bruneau, R. Purba, Special perforated steel plate shear walls with reduced beam section anchor beams. II: analysis and design recommendations, J. Struct. Eng. 135 (2009) 221–228. , http://dx.doi.org/10.1061/(ASCE)0733-9445(2009)135:3(221).

[7] M.M. Alinia, M. Dastfan, Behaviour of thin steel plate shear walls regarding frame members, J. Constr. Steel Res. 62 (2006) 730–738. , http://dx.doi.org/10.1016/j.jcsr.2005.11.007.

[8] M.M. Alinia, R. Sarraf Shirazi, On the design of stiffeners in steel plate shear walls, J. Constr. Steel Res. 65 (2009) 2069–2077. , http://dx.doi.org/10.1016/j.jcsr.2009.06.009.

[9] M.M. Alinia, M. Dastfan, Cyclic behaviour, deformability and rigidity of stiffened steel shear panels, J. Constr. Steel Res. 63 (2007) 554–563. , http://dx.doi.org/10.1016/j.jcsr.2006.06.005.

[10] S.A.A. Hosseinzadeh, M. Tehranizadeh, Introduction of stiffened large rectangular openings in steel plate shear walls, J. Constr. Steel Res. 77 (2012) 180–192. , http://dx.doi.org/10.1016/j.jcsr.2012.05.010.

[11] H. Valizadeh, M. Sheidaii, H. Showkati, Experimental investigation on cyclic behavior of perforated steel plate shear walls, J. Constr. Steel Res. 70 (2012) 308–316. , http://dx.doi.org/10.1016/j.jcsr.2011.09.016.

[12] A. Astaneh-Asl, Seismic behavior and design of steel shear walls, steel Technical Information and Product Service Report, Structural Steel Educational Council, Moraga, California, USA, 2001.

[13] B. Shekastehband, A. Azaraxsh, H. Showkati, Experimental and numerical study on seismic behavior of LYS and HYS steel plate shear walls connected to frame beams only, Arch. Civil Mech. Eng. 17 (2017) 154–168. , http://dx.doi.org/10.1016/j.acme.2016.09.006.

[14] A. Sahebjam, H. Showkati, Experimental study on the cyclic behavior of perforated CFRP strengthened steel shear walls, Arch. Civil Mech. Eng. 16 (2016) 365–379. , http://dx.doi.org/10.1016/j.acme.2016.01.009.

[15] ANSYS Release 12.1, Users guide manual, ANSYS Inc., Canonsburg, Pennsylvania, USA, (2012).

[16] AISC, Seismic Provisions for Structural Steel Buildings, ANSI/AISC 341-10, American Institute of Steel Construction, Chicago, Illinois, USA, 2010.

[17] S.P. Timoshenko, J.M. Gere, Theory of Elastic Stability, 2nd ed., McGraw-Hill Book Company, Mineola, NY, 1961.

[18] FEMA-356, Prestandard and commentary for the seismic rehabilitation of buildings, Federal Emergency Management Agency, Washington, D.C., USA, 2000.

[19] MATLAB and statistics Toolbox Release 2016b, User's Guide, The MathWorks Inc., Natick, Massachusetts, USA, 2016.